Photoinduced surface relief grating formation in amorphous $As_{40}S_{60-x}Se_x$ thin films

M.REINFELDE[a], L.LOGHINA[b], Z.G.IVANOVA[c], J.TETERIS[a], U. GERTNERS[a], S.SLANG[b], M.VLCEK[b]
[a]*Institute of Solid State Physics, University of Latvia, Kengaraga 8, Riga, Latvia*
[b]*Faculty of Chemical Technology, University of Pardubice, Studentska 95, Pardubice, Czech Republic*
[c]*Institute of Solid State Physics, Bulgarian Academy of Science, 72 Tzarigradsko Chaussee Blvd., 1784 Sofia, Bulgaria.*

The studies of direct holographic recording of the surface relief gratings (SRG) on amorphous $As_{40}S_{60-x}Se_x$ ($0 \le x \le 60$) thin films are presented. The gratings were created by orthogonally ±45° linearly polarized light beams of various wavelengths (λ = 473 - 650 nm). The surface structure of the relief gratings was investigated by atomic force microscopy. The influence of laser beam wavelength and spatial frequency of the gratings (grating period Λ) on the surface relief grating formation efficiency was examined.

(Received November 05, 2015; accepted February 10, 2016)

Keywords: Amorphous chalcogenide films, Holographic recording, Surface relief gratings

1. Introduction

The direct formation of surface relief grating (SRG) by two coherent laser beam interference has been studied in numerous disordered materials such as amorphous inorganic chalcogenides [1-4] and organic azobenzene compounds [5,6]. The efficiency of recording is determinate by distribution of electric field vector of resulting interference pattern inside the recording media [1,2]. Recently, chalcogenide As-S-Se glasses are extensively investigated as a promising medium for optical recording and lithography [7,8]. The formation of SRG in amorphous thin films strongly depends on the polarization state of the recording beams [2, 4, 9-11]. The results have shown that all illuminated volume of the film takes part in SRG formation process [12-15], and the largest SR modulation has been achieved with $+45^o$: $–45^o$ and RCP: LCP recording beam configurations. More profound studies show the SRG formation efficiency dependence on film thickness and grating period [13-15]. As one of the factors affecting this effect, we should take in account the interaction between surface tension and surface relief grating formation forces due to light intensity and electric field gradient parallel as well perpendicular to the film plane. So that should lead to the weakening of surface grating formation driving forces in the case of larger grating periods from one side and in the case of smaller light penetration depth at growing absorption from the other side [14]. Besides, the influence of higher order diffracted beams developing during the recording process inside the films volume when the light penetration depth is sufficiently large should not be excluded.

2. Experimental

The basic scheme for holographic SRG recording is shown in Fig.1.

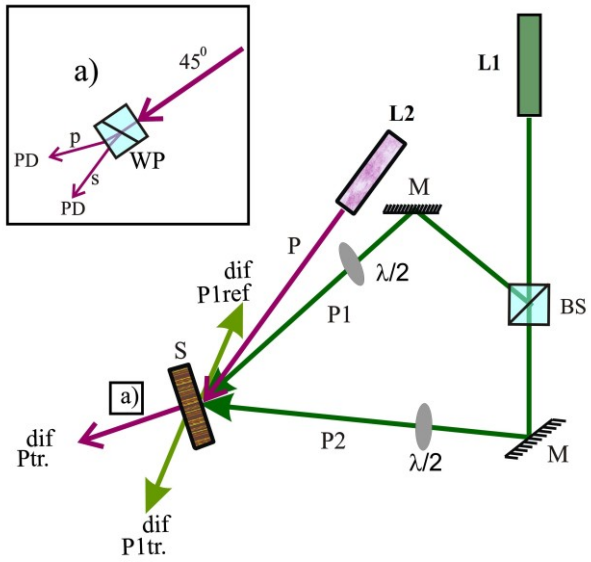

Fig.1. Recording scheme: L1 – recording and L2 probing lasers, P1,P2 – recording beams, P-probing beam, P^{dif}_{refl} and P^{dif}_{trns} – corresponding reflected and transmitted diffracted beams; BS-– beam splitter, M – mirrors, λ/2 – half-wave plates PD - photodiodes; WP –Wollaston prism

The SRG recording was performed with two orthogonally $+45^o$:$–45^o$ linearly polarized laser beams of

equal intensities I_1=I_2≈0,6 W/cm^2. Lasers with wavelength λ = 473 to 650 nm was used. SRG recording process was controlled by registration of the kinetics of reflected and transmitted diffracted light at the recording wavelength and using the non-destructive probing light beam. To show the relationship between SRG and polarization holographic grating formation we performed some experiments by splitting the transmitted diffracted light beam in two orthogonally polarized light beams using the Wollaston prism – shown in Fig.1, inset a). Accordingly, when 45^o polarized probe beam was used, transmitted diffracted light was divided into s and p polarized light beams. The SRG profile was examined by AFM after recording at constant illumination dose E≈13,5 kJ/cm^2.

In this article, studies on the direct surface structure formation by holographic recording of non-annealed $As_{40}S_{60-x}Se_x$ ($0 \le x \le 60$) thin films, prepared by thermal vacuum deposition on soda-lime glass substrates [16], are performed. The compositional dependences of SRG efficiency and corresponding recording kinetics are presented for grating period $\Lambda \approx 1.0$ μm and films thickness $d \approx 1$μm. The investigation of grating period Λ influence on SRG formation efficiency is performed as well. The grating period Λ has been changed by varying the angle between the recording beams. All experiments are carried out at room temperature.

3. Results and discussion

As we stated earlier [12], the main stage of SRG formation process is taking place after the film darkening by illumination [12]. The changes of the absorption coefficient and corresponding light penetration depth before (α_0, δ_0) and after (α_{fin}, δ_{fin}) illumination of the films (following Beer-Lambert law) have shown in Figs. 2 and 3. t The favourable conditions for SRG formation appear when α is near the 10^4 cm^{-1} and the corresponding δ values ~1μm or slightly below [14]. At first, it should be noted, that α values are decreasing and δ values increasing towards longer wavelength. From the other side, raising the Se content in the films compositions we can see the tendency in increasing of α and decreasing of δ. So, if x=0 (As_2S_3 composition) from our calculations α_{fin} = 6×10^3cm^{-1} for λ = 491 nm and α_{fin} =0,5 $\times10^3$ cm^{-1} for λ = 561 nm. When x is = 45 ($As_{40}S_{15}Se_{45}$ composition) α_{fin} = $8{,}4\times10^4$ cm^{-1} for λ = 491 nm and α_{fin} =4,7x10^3 cm-1 for λ = 633 nm. Consequently, δ_{fin}= 0,97 μm for λ = 491 nm are growing to δ_{fin}= 6,3 μm for λ =561 nm if x = 0 and δ_{fin} = 0,11μm for λ = 491 nm are growing to δ_{fin} = 1,11 μm for λ = 633 nm - if x =45.

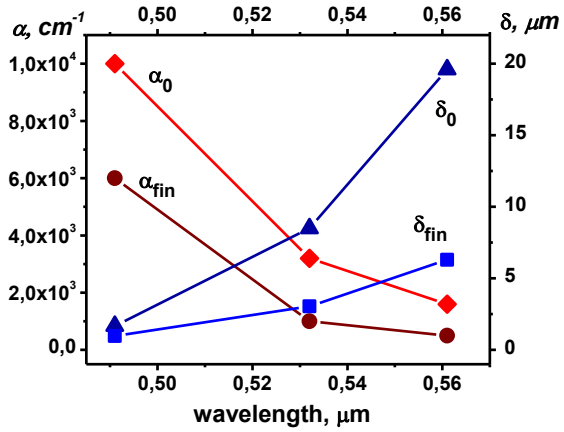

Fig. 2. Absorption coefficient α and light penetration depth δ of As_2S_3 film calculated for recording laser lines before (α_0, δ_0) and after (α_{fin}, δ_{fin}) illumination.

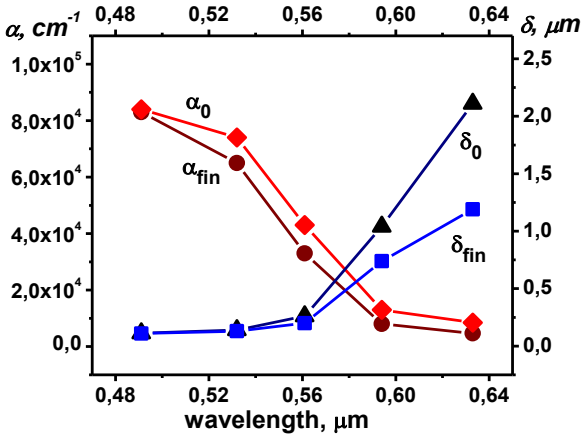

Fig. 3. Absorption coefficient α and light penetration depth δ of $As_{40}S_{15}Se_{45}$ film calculated for recording laser lines before (α_0, δ_0) and after (α_{fin}, δ_{fin}) illumination.

The dependences of surface relief profile depth (Δh) and the first order diffraction efficiency (η) on the Se-content (x, at.%) for recording laser beams are presented in Figs. 4 and 5. The results show that maximum values of $\Delta h \approx$ 170 nm and $\eta \approx$20 % are obtained at λ = 532 nm in the range of between 5-20 at.% Se. For the wavelengths of 630 and 650 nm at the recording condition as seen in Fig. 3, surface relief is almost unnoticeable or did not appears at all. Besides, the corresponding η values are very small or even zero (Fig. 4).

We also analyzed the obtained results from the point of view of the absorption coefficient α and the light penetration depth δ in Figs. 4 and 5. For of As_2S_3 films (x=0) the higher $\Delta h \approx$ 150 nm belongs to λ = 491 nm (α_{fin} = 0.6×10^4cm^{-1}, δ_{fin}= 0,97μm) and lower (Δh below 10 nm) – belong to λ = 594 nm (α_{fin} less than 0,5 $\times10^3$ cm^{-1}, δ_{fin} above 6,3 μm). Meanwhile for films, with Se content x

> 40, the optimal recording wavelength can be attributed to the optical range 532nm < λ < 594 nm (~$3x10^4 cm^{-1}$ < ~ α_{fin} < 0.8 $\times 10^4 cm^{-1}$, δ_{fin} ~ 0,13 to 0,7 μm). Therefore, the efficiency of SRG formation is limited by too low or too high absorption.

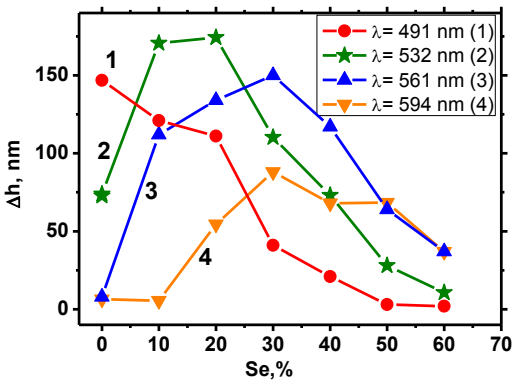

Fig.4. Relief profile height Δh dependence on selenium content (x) for $As_{40}S_{60-x}Se_x$ thin films for different recording laser wavelengths: film thickness d ≈ 1,0 μm, exposure dose E ≈ 13,4 kJ/cm², period of gratings Λ ≈ 1 μm.

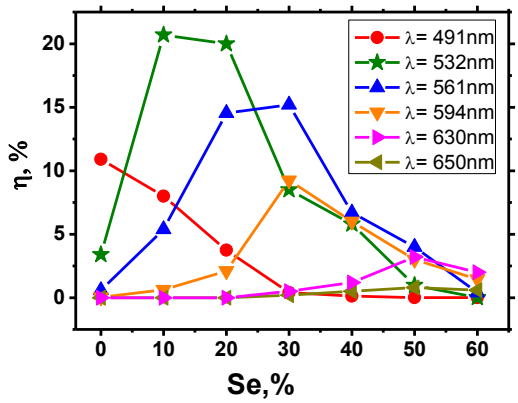

Fig.5. The first - order diffraction efficiency (η, %) dependence on selenium content (x) for $As_{40}S_{60-x}Se_x$ thin films for different recording laser wavelengths: film thickness d ≈ 1,0 μm, exposure dose E ≈ 13,4 kJ/cm², period of gratings Λ ≈ 1 μm.

Again we can get the conclusion that the favorable conditions for SRG formation appear when α is near the 10^4 cm^{-1} and corresponding δ values ~1μm or slightly below**.** From the dependencies on Fig.4, we can evaluate the optimal film content for given wavelength (for example: if λ = 491nm x_{opt}≈0, at λ = 532nm – ~10<$x_{opt,}$< ~20, etc.). Furthermore, considering fully thin film by laser beam of sufficiently strong intensity, [13], it is possible to choose the optimal film thickness.

The results of detailed study for the influence of the grating period Λ on SRG formation by 594 nm laser recording are shown in Fig. 6. The relief depth up to 550 nm is obtained for a period of Λ = 4.8 μm. AFM scan in Fig. 7 illustrates the relief depth for Λ =3,59 μm. The dependency curves indicate the existence of an optimal grating period at Λ_{opt} ~ 5 μm at the stated illumination dose E. The profile height Δ*h* has a maximum value, while falling down versus smaller and greater periods for the same value of *E*. According to [14], the grating period affects the SRG formation efficiency.

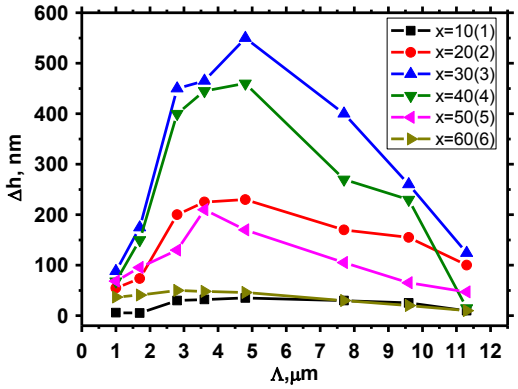

Fig.6. Relief profile height Δh, with grating period Λ, μm for $As_{40}S_{60-x}Se_x$ thin films: film thickness d ≈ 1,0 μm, exposure dose E ≈ 13,5 kJ/cm², x – selenium content, at%, recording laser wavelength λ = 594 nm

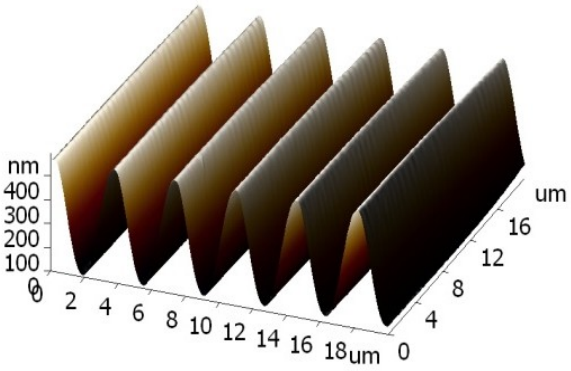

Fig.7. AFM scan of the $As_{40}S_{30}Se_{30}$ SRG formed by the exposure of a 594 nm wavelength laser beam: film thickness d ≈ 1,0 μm, period Λ=3,59, exposure dose E = 13,5 kJ/cm².

The value of Λ_{opt} for holographic recording of SRGs with orthogonally ±45° linearly polarized light beams depends on the film thickness and exposure dose. The reason for the existence of Λ_{opt} could be related to possible equilibrium state between the surface tension and SRG formation forces, which are originated by the light intensity gradient parallel to grating vector.

In a previous paper [10], the detailed course of SRG hologram recording kinetics and presence of vector polarisation hologram in $As_{40}S_{15}Se_{45}$ films by light illumination at λ = 633 nm has been described. Fig. 8

illustrates such a characteristic pattern of SRG formatting process in $As_{40}S_{30}Se_{30}$ films under λ = 532 nm light illumination, where two different areas in hologram recording curves can be distinguished. At the beginning when exposition $E \approx 13{,}5$ J/cm^2 the diffraction efficiency achieves certain maximum. Inset, A in Fig. 8 shows the magnification of recording kinetics first 2 min. (with η_{max} ≈0,02%) of the recording process . After short decrease, the values of diffraction efficiency increase again and approach to saturation near the $E \approx 13{,}5$ kJ/cm^2. That second recording stage corresponds to surface relief formation. The polarisation status of diffracted beam was fixed by separating p and s polarized light using the Wollaston prism.

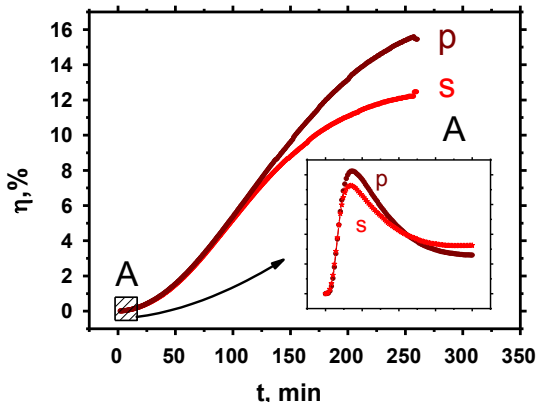

Fig. 8. SRG recording kinetics: p and s - polarization of diffracted light divided by Wollaston prism, recording light λ1=532 nm, intensities I1=I2 ≈ 0,9 W/cm^2, probing light λ2=672 nm, polarisation 45^o, intensity I ≈ 15 mW/cm^2, $As_{40}S_{50}Se_{10}$ film thickness d=1μm; grating period Λ= 1 μm).

4. Conclusion

The direct surface relief gratings formation in thin films of chalcogenide semiconductor $As_{40}S_{60-x}Se_x$ ($0 \le x \le 60$) compositions at laser illumination wavelengths λ = 473, 491, 561, 532, 594, 630 and 650 nm was studied. The obtained results can help to optimize wavelengths for holographic recording of surface relief gratings with orthogonally ±45° linearly polarized light beams in $As_{40}S_{60-x}Se_x$ thin films in dependence of film composition.

Analysis of the relationships between the light penetration depth in the films and optimal conditions for SRG can point to choice of favourable film thickness. In this context we can judge that films with thickness d=1μm used in our studies might be close to the optimum value.

Acknowledgments

Authors[2] acknowledge project No. CZ.1.05/4.1.00/11.0251 "Center of Materials and Nanotechnologies" co-financed by the European Fund of the Regional Development and the state budget of the Czech Republic.

References

[1] A. Saliminia, T.V. Galstian, A .Villeneuve, Phys.Rev. Lett. **85,** 4112 (2000).
[2] K. E. Asatryan, T. Galstian, R. Vallee, Phys. Rev. Lett. **94,** 087401 **(**2005) .
[3] S. Kokenyesi , I. Ivan , V. Takats, J. Palinkas, Biri S,. I. A. Szabo, J. Non-Cryst. Solids **353,** 147 (2007).
[4] U. Gertners, J. Teteris, Opt. Mat., **32,** 807 (2010).
[5] P. Rochon, E. Batalla, A. Natansohn, Appl. Phys. Lett. **66,** 136 (1995).
[6] B. Bellini, J. Ackermann, H. Klein, Ch. Graves, Ph. Dumas, V. Safarov, J. Phys.: Cond.Matter **18,** 1817 (2006).
[7] M. Vlcek, S. Schroeter, S. Brueckner, S. Fehling A. Fiserova, J. Mater. Sci.: Materials in Electronics **20,** 290 (2009).
[8] J. Teteris, M.Reinfelde J. Non-Cryst.Solids **353**, 1450 (2007).
[9] V. M. Kryshenik, M. L. Trunov, V.P. Ivanitsky J. Optoelectron. Adv. M. **9,** 1949 (2007).
[10] M. Reinfelde, J. Teteris, J. Optoelectron. Adv. M. **13,** 1531 (2011).
[11] J. Teteris, U. Gertners, M..Reinfelde, Phys. Status Solidi C **8,** 2780 (2011).
[12] M. Reinfelde, R. Grants, J. Teteris, J Phys. Status Solidi C **9**(12), 2586 (2012).
[13] M. Reinfelde, J. Teteris J. Non-cryst. Solids **377,** 162 (2013).
[14] M. Reinfelde, J. Teteris, E Potanina Canad. J. Phys. **92,** 659 (2014).
[15] J. Teteris, U. Gertners, IOP Conf. Series: Mat. Sci. Engineering **38,** 012012 (2012).
[16] L. Loghina, J. Teteris, M. Vlcek, Photoptics, Proceedings **1,** 121 (2015).

*Corresponding author: mara.reinfelde@cfi.lu.lv